

Infrared spectral energy distribution of four star forming regions

A. D. Karnik¹, S. K. Ghosh¹, T. N. Rengarajan¹, S. N. Tandon² and R. P. Verma¹

¹ Tata Institute of Fundamental Research, Homi Bhabha Road, Mumbai 400005, India

² Inter University Centre for Astronomy and Astrophysics, Pune 411007, India

Abstract. Star forming regions associated with IRAS 19181+1349, 20255+3712, 20178+4046 and 10049+5657 have been mapped simultaneously in two far infrared bands ($\lambda_{\text{eff}} \sim 130$ and $210 \mu\text{m}$), using TIFR 1m balloon borne telescope with liquid ³He cooled bolometer arrays. HIRES processed IRAS maps at 12, 25, 60 and 100 μm have been compared with ours. The TIFR maps show much more structural details due to their superior angular resolution. Detail radiation transfer modelling has been carried out for each of these sources and compared with observed spectral energy distributions.

Key words : infrared emission — star formation — molecular cloud

1. Introduction

As part of an ongoing program to map cool dust in Galactic star forming regions using TIFR 100 cm balloon-borne far infrared (FIR) telescope four star forming regions associated with IRAS 19181+1349, 20255+3712, 20178+4046 and 10049+5657 were simultaneously mapped using a two band photometer with $\lambda_{\text{eff}} \approx 130$ and $210 \mu\text{m}$. (for 30 K greybody with emissivity law λ^{-1}). The two band photometer consists of composite ³He cooled Si bolometer arrays in 3x2 configuration and Winston cones in front of each bolometer defines the FOV to be $1.6'$.

2. Observations and data reductions

The observations were performed on 20 February 1994 during the flight of the TIFR 100 cm balloon borne far infrared telescope. Sources were simultaneously raster scanned in two FIR bands with the telescope beam chopped at 10 Hz with $\sim 4'$ amplitude in the scan direction. The data were deconvolved using an inhouse developed scheme, based on maximum entropy

method (MEM), to generate high angular resolution ($\sim 1'$ maps at 130 and 210 μm (Fig. 1). Flux calibration was performed using Jupiter observed twice during the flight.

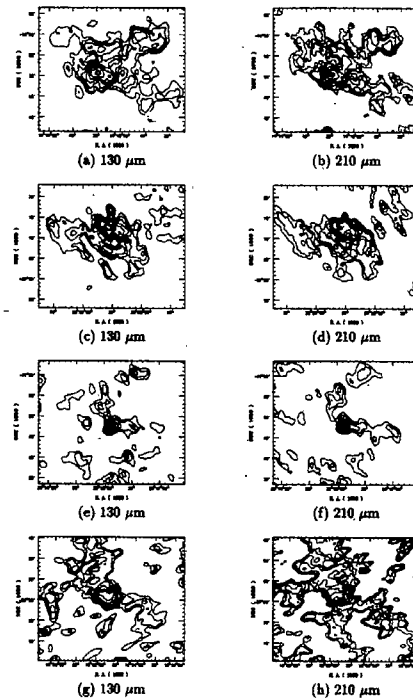


Figure 1. Infrared maps of IRAS 19181+1349 for a) 130 μm b) 210 μm , of IRAS 20255+3712 for c) 130 μm d) 210 μm , of IRAS 20178+4046 for e) 130 μm f) 210 μm , and of IRAS 10049-5657 for g) 130 μm h) 210 μm . Contours are drawn at 1.0, 2.5, 5, 10, 20, 40, 80, 95 percent of peak intensities which are 867, 189, 1578, 533, 2067, 622, 1056, 311 Jy/sq. arc min respectively.

The IRAS survey data in four bands (12, 25, 60 and 100 μm) for the same regions were HIRES processed at IPAC (Caltech) for comparison. Better structural information is available in the TIFR maps than in the IRAS-HIRES maps (not presented in this paper).

The observed flux densities in six wavebands (in $3'$ dia aperture) were used along with the available IRAS LRS data to construct infrared spectral energy distributions (SED).

3. Radiation transfer modelling

Radiation transfer calculations for a self consistent model assuming a spherically symmetric dust envelope around an embedded star are carried out using code CSDUST3 (Egan et al., 1988). The dust was assumed to be a mixture of Graphite, Astronomical Silicate and Silicon Carbide grains. Absorption and scattering efficiencies, Q_{abs} , Q_{sca} and scattering anisotropy factor g were used as per Laor and Draine (1993). Size distribution of all the three types of grains was assumed to be of a power law form ($n(a) \approx a^{-3.5}$) as per Mathis, Rumpl & Nordsieck (MRN) (1997) and averages of Q_{abs} , Q_{sca} and g over size distribution are used as

input to the model. Luminosity computer from the available SED was used as total luminosity of the central source. Parameters of the model include the size of the envelope, line of sight optical depth at 100 μm , dust composition, radial density distribution ($n(r) \propto r^0, r^{-1}, r^{-2}$).

Uniform density distribution gives the best fit (Fig. 2) for all the four sources. Other parameters yielding best fits are presented in Table 1.

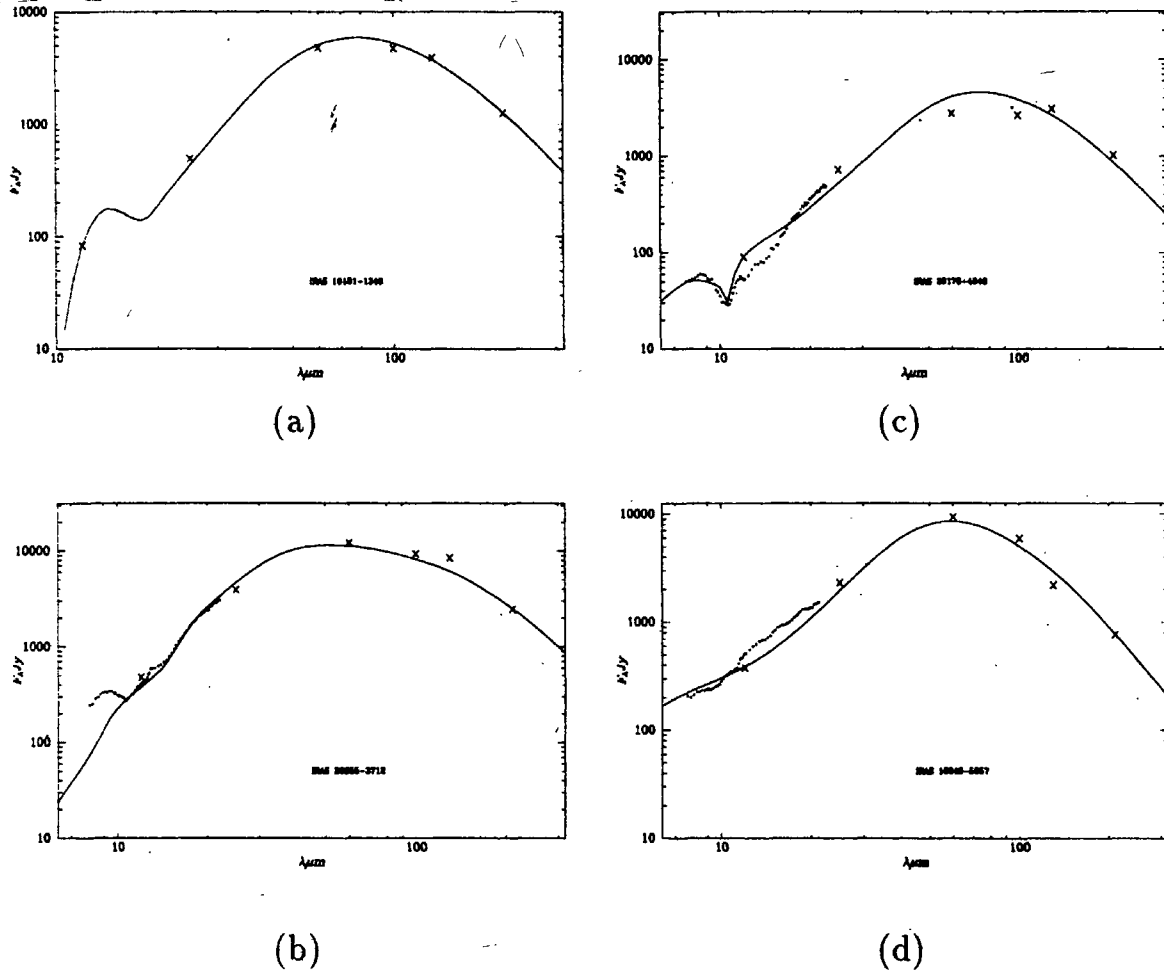


Figure 2. Model fits to SED of a) IRAS 19181+1349, b) IRAS 20255+3712, c) IRAS 20178+4046 and d) IRAS 10049-5657. Smooth line represents radiation transfer model predictions; crosses and dots represent observed flux densities.

Table 1. Radiation transfer model parameters yielding best fits to observed SEDs.

Source	D(kpc)	L(L _⊙)	R _{envelope} (pc)	$\tau_{100\mu\text{m}}$	Dust composition C:Si:SiC
IRAS 19181+1349	9.7	1.16E+06	1.8	0.062	20:80:0
IRAS 20255+3712	2.3	1.95E+05	5.0	0.002	60:40:0
IRAS 20178+4046	3.3	9.74E+04	0.3	0.14	92:3:5
IRAS 10049-5657	7.1	1.14E+06	0.6	0.09	100:0:0

Conclusions

TIFR maps at 130 and 210 μm show much more structural information compared to IRAS-HIRES maps. We attempted to model these sources assuming spherical symmetry. Radiation transfer models fit better for uniform density dust envelope for all sources.

IRAS 19181+1349 SED matches well with uniform density distribution. As there was no LRS spectra available for the source one can't comment about the dust composition though there seems to be a silicate feature present which manifests in the 12 μm flux and amorphous silicate with Graphite dust envelope matches well with observations.

IRAS 20178+4046 LRS spectra shows strong absorption at 10.6 μm but much broader than possible with Graphite+SiC (10.6 μm feature) mixture alone, which was modelled assuming mixture of Graphite, Astronomical Silicate (9.7 μm feature) and SiC. This suggests that in Carbon rich environment amorphous silicate is equally abundant as Silicon Carbide.

IRAS 20255+3712 LRS spectra also shows absorption at 10.6 μm . It is possible to match this feature if SiC is abundant near outer edges of envelope.

IRAS 10049-5657 LRS spectra is featureless and model with only carbon dust matches well with observations.

References

- Egan M. P., Leung C. M., Spagna Jr. G. F., 1988, *Computer Physics Communications*, 48, 271.
Laor A., Draine B. T., 1993, *ApJ*, 402, 441.
Mathis J. S., Rumpl W., Nordsieck K. H., 1977, *ApJ*, 217, 425.